Int. J. Solids Structures Vol. 29, No. 14/15, pp. 1957–1968, 1992
Printed in Great Britain.

0020–7683/92 $5.00 + .00
Pergamon Press plc

A UNIFIED APPROACH OF FRACTURE AND DAMAGE MECHANICS TO FATIGUE DAMAGE PROBLEMS

HAJRUDIN PAŠIĆ
Department of Mechanical Engineering, The University of Sarajevo, 71000 Sarajevo, Yugoslavia

Abstract—The paper demonstrates how combined fracture and damage mechanics may be used to establish a fatigue damage model for polycrystalline materials in a stress-controlled test. Damage is defined as the product of the longest or "equivalent" surface crack length and the accumulated strain range, both taken with certain exponents which are found from loading conditions and failure criterion. The short to long crack transition is described through El Haddad's redefined stress intensity factor at threshold, while the failure is determined by the behaviour of the major crack.

The quality of the results is encouraging. Even though some partial comparisons with already published results are presented, the model is yet to be subjected to more extensive experimental verification.

1. INTRODUCTION

Fatigue crack propagation and fatigue damage of structural components have become subjects of unquestionable relevance. However, most of the research efforts are separated into several fields such as fracture mechanics, damage mechanics, fatigue etc., while combined efforts are missing. This paper presents an essential part of the results of an attempt at such combination (Pašić, 1990).

A large part of the fatigue life of metallic structures is related to a sequence of processes during which localized strains, slip bands and microcracks initiate and develop until the macroscopic crack that leads to fracture is formed. The life is therefore controlled by a complex crack-growth phenomenon (Kitagawa *et al.*, 1979; Suh *et al.*, 1985, 1990; Magnin *et al.*, 1989). It is very difficult to describe analytically this progressive material deterioration and growth of individual cracks and their systems. Therefore, some global measures are needed for description of these processes. On this line many analytical models have been developed (see for example Collins, 1981). Unfortunately, most of them are purely phenomenological.

Depending on the point of view of the authors of fatigue–failure models which pretend to be based on physical grounds, they are founded on either microscopic or macroscopic variables. The first type is based on a crack length as a critical variable (Miller and de los Rios, 1986), while the second one uses a damage variable as a global measure of the material degradation (Chaboche, 1988). The first approach is an attempt to extend the application of fracture mechanics to very short cracks, while the second one is an attempt to generalize continuum damage mechanics (Lemaitre and Chaboche, 1984; Krajcinovic and Lemaitre, 1987). In fact, as shown by Cailletaud and Levaillant (1984) there could be implicit connections between the continuous damage parameterization and the crack length used in fracture mechanics. The model developed here may be considered as a combination of those models.

To bridge the gap the first step is a mathematical description of short to long crack transition at threshold in terms of number of cycles. Next, damage is defined as the product of the longest surface crack length and the accumulated strain range, both taken with certain exponents which are to be found from loading conditions, failure criterion etc. The quality of the results is encouraging.

2. SHORT TO LONG CRACK TRANSITION

Long cracks are monitored in LEFM-type specimens in such a way that a crack is inserted in a specimen before testing. The initial crack length is typically a few millimeters long and its further growth is obtained by integrating the crack growth rate described by the Paris Law (Hertzberg, 1988):

$$\frac{da}{dN} = C_1 \Delta K^m \tag{1}$$

where C_1 and m are the material constants, N is number of cycles and ΔK is the stress intensity factor range

$$\Delta K = C_2 \Delta\sigma \sqrt{\pi a}, \tag{2}$$

where $\Delta\sigma$ and C_2 are the applied stress range and the crack geometry constant.

However, many engineering components do not contain big flaws such that the period of the first crack development may consume an important part of its life before the crack becomes long. It has also been found that under the same driving force the growth rates of short cracks are greater than the corresponding rates of long cracks (Miller, 1982; Miller and de los Rios, 1986; Suresh and Ritchie, 1984). This suggests that the use of data for long cracks in defect-tolerant lifetime predictions for structural components can lead to considerable overestimates. Interpretations of big differences between large endurance limits of plain specimens and low endurance limits of notched specimens have not become possible until recently because of the lack of information on the short crack behaviour (Miller, 1987).

Recognizing the fact that the short crack behaviour requires an elastoplastic analysis, Kitagawa and Takahashi (1976) have proposed a single approach that combines both LEFM and EPFM at threshold (Fig. 1). The line given by ΔK_{th} represents the long crack threshold condition. But for shorter cracks to propagate, higher loads must be applied and small scale yielding conditions for validity of LEFM violated. This happens to be the case when $\Delta\sigma$ exceeds about 2/3 of the cyclic yield stress σ_{cy} in a reversed stress test (when the stress ratio is $R = -1$). The horizontal bounding line in the diagram is the fatigue limit of the plane specimen $\Delta\sigma_e \cong \Delta\sigma_{cy}$. The shaded area in Fig. 1 corresponds to the so-called microstructurally short nonpropagating cracks (MSC). Experimental studies indeed clearly show that threshold stresses for long and short cracks are different (Tanaka *et al.*, 1981), and the Kitagawa–Takahashi diagram shows that the threshold condition for long crack

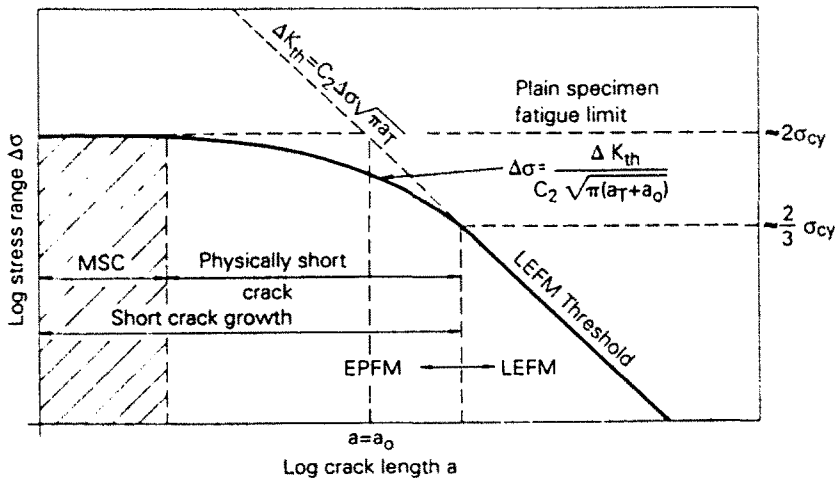

Fig. 1. Kitagawa–Takahashi diagram for short and long cracks.

propagation is a constant stress intensity, while the same condition for short cracks is a constant stress $\Delta\sigma_e$.

In rationalizing the behaviour of long and short cracks with respect to the threshold condition, El Haddad *et al.* (1979) proposed redefinition of the stress intensity factor, such that for both long and short cracks at threshold (Fig. 1):

$$\Delta K = C_2 \Delta\sigma \sqrt{\pi(a+a_0)} \tag{3}$$

instead of eqn (2). The so-called intrinsic crack length a_0 is then obtained from eqn (3) from the condition that $\Delta\sigma$ tends to $\Delta\sigma_e$ as the crack length a approaches zero (Fig. 1), therefore being

$$a_0 = \frac{1}{\pi}\left(\frac{\Delta K_{th}}{\Delta\sigma_e}\right)^2. \tag{4}$$

The new definition is a completely empirical one since the parameter a_0 has no physical significance. On the other hand, Tanaka and co-workers (1981) have shown that El Haddad's approach is a special case of their slip band model, such that, in this light, El Haddad's model may be viewed as not being purely empirical—see also Suresh and Ritchie (1984). The earliest crack growth experiments had shown that in general da/dN versus ΔK curves are of the form shown in Fig. 2, and that the Paris Law, eqn (1), does not hold at threshold—below which cracks do not grow or grow very slowly, say at rates of the order of 10^{-10} m/cycle. Empirically, growth rates in that region can be described as (Allen *et al.*, 1988):

$$\frac{da}{dN} = C_1(\Delta K - \Delta K_{th})^m, \tag{5}$$

where the value ΔK_{th} strongly depends on the mean stress, i.e. the load ratio R. Xiulin (1987) shows the applicability of eqn (5) with $m = 2$ to such diverse materials as b.c.c. high-strength low-alloy steels, f.c.c. aluminum and h.c.p. titanium alloys.

In the threshold region sizes such as the plastic zone or the crack tip openings are of the same order as the microstructural features such as grain size, for example. Therefore the crack growth mechanisms and growth rates at threshold are strongly influenced by the microstructure. At the transition point $\Delta K = \Delta K_t$ (Fig. 2), the crack growth rate curve starts to deviate from the straight line in the logarithmic plot. Below $\Delta K = \Delta K_t$ the growth rate decreases rapidly and the crack stops its propagation at threshold. Liu and Liu (1982, 1984) examined fifty fatigue crack propagation data for steels and aluminum alloys and found the empirical relation

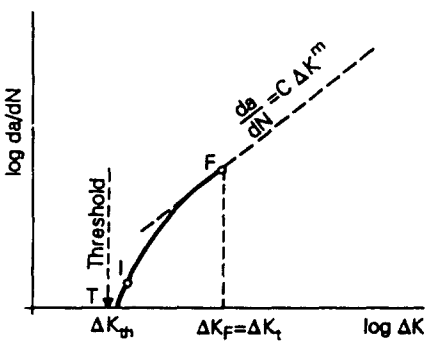

Fig. 2. Fatigue crack growth rate versus stress intensity range.

$$\Delta K_{th} = (0.7 \mp 0.1)\Delta K_t. \tag{6}$$

In the threshold region when the cyclic plastic zone size r_c is of the grain size, the microstructural features such as grain boundaries serve as dislocation barriers and impede plastic deformation. Yoder *et al.* (1982) suggested that at the transition point $r_c = \bar{l}$ where $\bar{l}$ is the mean free path of dislocation movement which is, for many materials, of the grain size. In the hypertransitional region $r_c > \bar{l}$ and a structure-insensitive or continuum mode of crack growth results. In their "unzipping model" Liu and Liu (1982) have shown that at $\Delta K < \Delta K_t$ the shear decohesion, by which the fatigue crack grows, is caused by the combined effects of stress relaxation and cyclic creep. In Liu and Liu (1984) the same authors took the net driving force as proportional to $(\Delta K - \Delta K_{th})^m$, such as in eqn (5), with $m = 2$ as in Xiulin (1987). It is very interesting that Navarro and de los Rios (1987), applying the crack model of Bilby, Cottrell and Swinden have also analytically derived eqn (6) with no adjustable parameters!

Starting with the new definition (3) for the stress intensity factor at and close to threshold, then using eqns (4) and (5) and introducing:

$$p = a_T + a_0, \quad r = a_F - a_T, \quad q = \frac{p}{r}, \quad \mathbf{a} = \frac{a - a_T}{r}, \quad \mathbf{a}_0 = \frac{a_I - a_T}{a_F - a_T}, \tag{7}$$

where the indexes F, T and I stand for crack lengths at "failure", "threshold" and "initial" (Fig. 2), such that the normalized crack length $\mathbf{a}_0 \leqslant \mathbf{a} \leqslant 1$, the following crack growth equation results:

$$-\mathrm{d}\mathbf{a} = A_m(\sqrt{\mathbf{a}+q} - \sqrt{q})^m \,\mathrm{d}N, \tag{8}$$

where

$$A_m = C_1(C_2\sqrt{\pi})^m r^{m/2-1}\Delta\sigma^m. \tag{9}$$

Double integration of (8), once from the initial crack length $\mathbf{a}_0$ to an arbitrary crack length $\mathbf{a}$ while the number of cycles runs from N_I to N, and the second time, when $\mathbf{a}_I < \mathbf{a} < 1$ while $N_I < N < N_F$ (Fig. 2), and taking $N_I = 0$, one obtains:

$$N = \frac{1}{B_m}(f(\mathbf{a}) - f(\mathbf{a}_0)) \tag{10}$$

$$N_F = \frac{1}{B_m}(f(1) - f(\mathbf{a}_0)). \tag{11}$$

Therefore the normalized life is:

$$\frac{N}{N_F} = \frac{f(\mathbf{a}) - f(\mathbf{a}_0)}{f(1) - f(\mathbf{a}_0)}, \tag{12}$$

where, depending on the coefficient m:

(a) if $m = 2$,

$$B_m = A_m/2, \quad f(\mathbf{a}) = \ln\left(\sqrt{\mathbf{a}+q} - \sqrt{q}\right) - \sqrt{q}/\left(\sqrt{\mathbf{a}+q} - \sqrt{q}\right);$$

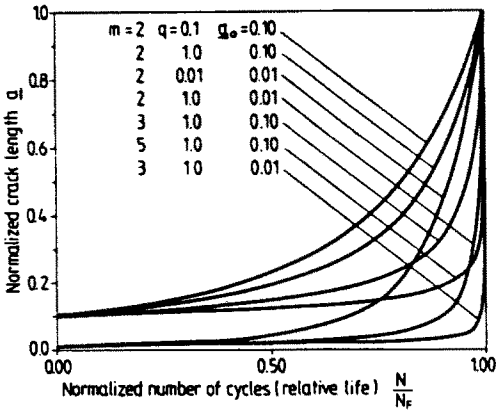

Fig. 3. Normalized crack length versus normalized life.

(b) if $m = 2$

$$B_m = A_m \frac{(m-1)(m-2)}{2}, \quad f(\mathbf{a}) = \frac{(1-m)\sqrt{\mathbf{a}+q}+\sqrt{q}}{(\sqrt{\mathbf{a}+q}-\sqrt{q})^{m-1}}.$$

Equation (12) could be numerically solved for the set of parameters m, $\mathbf{a}_0$ and q, and an example of such a calculation is shown in Fig. 3.

A typical value for q may be judged from eqns (3), (6) and (7). Namely, identifying the point F (failure) with the transition point (Fig. 2), eqn (6) leads to $\Delta K_{th}/\Delta K_F = 0.7$. Taking $0.7^2 \cong 0.5$ it follows that $a_F = 2a_L + a_0$ and $q = 1$. Integration of eqn (8) beyond the transition point does not change the specimen life significantly. For example, Hobson (1982) simply takes $a_F = 1$ mm: the length normally considered to correspond to long cracks. Therefore the value $q = 1$ seems to be reasonably well estimated.

3. DAMAGE MODEL

Let us assume that the series of stress-controlled experiments is made on several specimens at different stress levels but for all them cycled up to the same number of cycles (Fig. 4). As the number of cycles N is increased from $N_0 = 0$ to $N = N_F$ at failure, the stress–strain diagram due to fatigue-creep strain accumulation will be of the form shown in Fig. 5. Assuming that the stress range exceeds its value at threshold ($\Delta\sigma_T$), the specimen will eventually be broken for any $\Delta\sigma > \Delta\sigma_T$ sooner or later, depending on stress level after N_F cycles (Fig. 5).

Let us further assume that beyond the threshold (T) the strress–strain dependence, at a certain (constant) number of cycles N in a stress-controlled experiment may be described by (Fig. 5):

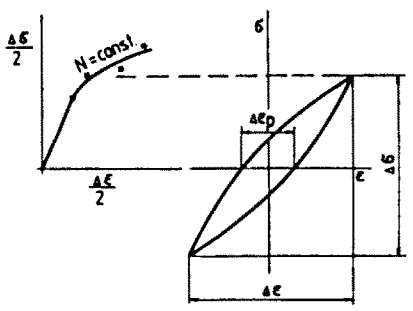

Fig. 4. Cyclic stress–strain range curve for N = const.

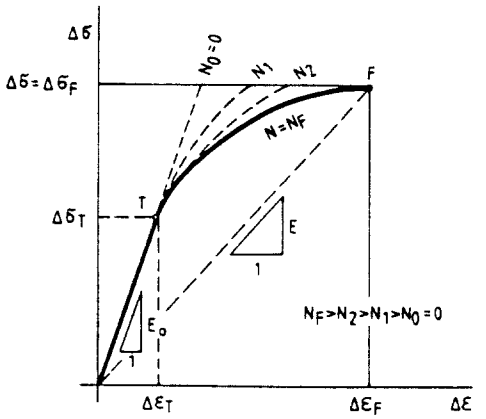

Fig. 5. Fatigue creep strain accumulation.

$$\Delta\sigma = E_0(1-D)\Delta\varepsilon, \tag{13}$$

where $\Delta\sigma = \Delta\sigma - \Delta\sigma_T$ is applied (constant) stress range beyond threshold, $\Delta\varepsilon(N) = \Delta\varepsilon(N) - \Delta\varepsilon_T$ is total strain range beyond threshold, $D = D(N)$ is damage, E_0 is virgin material Young's modulus. $E = E_0(1-D)$ may be considered as being the new modulus of damaged material (Fig. 5).

Next, let us define the damage. Fatigue damage mechanisms are very complex but they generally start at the surface of the material. The crack initiation is closely related to the localized strain produced by cycling and then, depending on the microstructure, various mechanisms take place up to the failure. The possible crack sites are found to be persistent slip bands (PSB), second-phase particles or, less frequently, at grain boundaries.

Liu *et al.* (1990) have recently studied surface fatigue damages in polycrystalline copper plain specimens at intermediate total strain levels (between low- and high-cycle fatigue). They found three types of damage: slip bands and twin and grain boundary microcracks, the great majority of which were confined to surface grains. Even in the intermediate region the life fraction to nucleate a surface crack of the three-grain-facets length was 75% to 90%, suggesting that a large fraction of the life is spent in nucleating a fatal crack on the surface. Finally, they found that at higher strain amplitudes fatal cracks are predominantly intergranular, while at low strain amplitudes most of the fatal surface cracks are formed by linking the transgranular PSBs in the adjoining grains by grain boundary cracks.

The crack development into the depth of polycrystalline materials commonly follows two distinct phases: (a) Stage I (Mode II, or shear mode) corresponds to the development of very small cracks within the few surface grains, following the PSBs in the maximum shear stress direction, and (b) Stage II (Mode I, striation mode) characterized by faster growth of a few microcracks that propagate transgranularly faster than the others in a plane perpendicular to the applied stress direction. The appearance of such a long crack corresponds to the failure of the loaded component. Fracture mechanics approaches cannot be applied to the evaluation of the growth behaviour of Stage I cracks. Brown and Ogin (1985) have found that the volume fraction of PSBs (associated with Stage I cracks), is closely related to the applied strain amplitude for variety of polycrystalline materials.

The early growth of short fatigue cracks in polycrystalline materials follows the pattern of repeated surface crack nucleation and linkage, since near the free surface the PSBs produce very large (with a logarithmic singularity) surface stresses with localized plastic flow (Brown and Ogin, 1985). Macroscopic internal stresses in PSBs change sign every half-cycle and the resulting shear stress between the band and the matrix always acts to increase slip near one side of the PSB, i.e. assists dislocation flow and the Stage I crack nucleation.

It has long been known that damage in high-cycle fatigue is influenced by both surface crack lengths and surface crack density (Kitagawa *et al.*, 1979; Suh *et al.*, 1985, 1990). Final fracture occurs by coalescence of many randomly distributed microcracks (not by

growth of a single crack), but is governed almost exclusively by the behaviour of the major crack. However, Polak and Liskutin (1990) show that the same crack need not remain the longest one within the whole fatigue life. Therefore, the authors have defined "equivalent crack length" which is close to the temporary largest crack length with the growth rate similar to one in Fig. 3. This crack length can be obtained if several cracks in one specimen are grown independently, or alternatively by averaging the dependence of the longest cracks on the cycle number measured in different specimens cycled at the same strain amplitude.

Having in mind the preceding discussion the damage model adopted here should include the longest surface crack or the averaged "equivalent crack length" as an important parameter; from now on it will be assumed that this crack grows in accordance with the rules described in Section 2 and eqn (12). Since the final fracture is governed by the behaviour of the major crack the failure criterion will be the one when crack length reaches the transitional length, i.e. when $\mathbf{a} = 1$.

As has already been discussed, fatigue damage is influenced by the surface crack density. On the other hand the crack density is a function of the volume fraction of PSBs and, as shown by Brown and Ogin (1985), is closely related to the applied strain amplitude. Realizing the importance of slip band formation, Kitagawa and co-workers (1979) measured slip line distribution and their density for several mild steels and one high-strength steel. They defined the so-called slipped-grain ratio of the slipped grains to the number of total surface grains. The important finding is that the slipped-grain ratio is proportional to the plastic strain range $\Delta\varepsilon_p$ and that the macroscopically measured strain (or stress) range seems to express the rate of local slips on the cyclically strained surface. Having all this in mind, let us define damage as:

$$D = \gamma \mathbf{a}^k \Delta\varepsilon^n, \tag{14}$$

where γ is a constant while $\Delta\varepsilon$ is a total strain rate beyond its threshold value (see eqn (13)). A similar form for damage, namely the product of the average flaw length and their number per unit volume is a characteristic measure of the loss of stiffness of brittle solids as well—see Budiansky and O'Connel (1976) and Laws and Brockenbrough (1987), for example. Socie *et al.* (1983) have discussed a variety of forms by which the damage parameter may be defined, such as in terms of the relative surface crack length $D = a/a_F$; in terms of stress drop in a strain-controlled test; or in terms of transient strain response in a stress-controlled test. In this light the damage model for the stress-controlled test described by eqn (14) may be viewed as being a combination of the first and the third of these forms.

Hua and Socie (1984) have evaluated four different damage theories in both high- (HCF) and low-cycle fatigue (LCF) regimes in 1045 steel under constant amplitude biaxial loading. They found that in the LCF region ($N_F < 10^4$) a number of damage nuclei were observed and that continuum damage theories should be applicable to this life regime. They also found that the surface-crack density parameter plays an important role but that this parameter alone is not a suitable measure for damage. On the other hand, in the HCF region a single dominant crack was used to represent fatigue damage, and continuum damage models, such as Chaboche's, "are not expected to model the life regime dominated by the growth of a single large crack". It has also been concluded that the HCF regime "none of the models can predict crack growth during the entire fatigue life" and, therefore "surface crack length definitely cannot be used as a damage parameter". This discussion also suggests that a damage model having the form (14) could be a compromising solution, because it includes both the longest crack length and crack density parameters.

The continuous damage models applied to fatigue processes have certain deficiencies. First, due to its surface character damage is heterogeneously distributed and, second, during the propagation period the number of large defects is small—at least in the last period of life—which is inconsistent with a continuum approach. However, in spite of this, CDM has been found to be a powerful tool in describing these complicated phenomena (Chaboche, 1988). It is interesting to note that Popelar and Hoagland (1986) have found the damage model such as the one described by (13), where D is assumed to be linearly proportional to the strain, may even be used to analyze the fracture of a double-cantilever-beam specimen

(with a single crack) and may successfully bridge the fields of damage and fracture mechanics.

4. RESULTS

From eqns (13) and (14) the stress–strain relationship reads:

$$\Delta\sigma = E_0(1-\gamma \mathbf{a}^k \Delta\varepsilon^n)\Delta\varepsilon, \tag{15}$$

while the stress and damage are related as:

$$\Delta\sigma = E_0(\gamma \mathbf{a}^k)^{1/n}(1-D)D^{1/n}. \tag{16}$$

For a fixed value of the crack length **a** Figs 6 and 7 depict eqns (15) and (16) for several values of the yet unknown parameter n.

Extreme values for the curves in Figs 6 and 7 are found from eqns (15) and (16) such that the damage, strain range and stress range at failure ($\mathbf{a}_F = 1$) are:

$$D_F = \frac{1}{n+1} \tag{17}$$

$$\Delta\varepsilon_F = \gamma^{-1/n}(n+1)^{-1/n} \tag{18}$$

$$\Delta\sigma_F = E_0\gamma^{-1/n}\frac{n}{(n+1)^{n+1/n}}, \tag{19}$$

while from eqns (16)–(18) there follows:

$$\gamma = \left(\frac{E_0}{\Delta\sigma}\right)^n \frac{n^n}{(n+1)^{n+1}} \tag{20}$$

$$\Delta\varepsilon_F = \frac{\Delta\sigma}{E_0}\frac{n+1}{n}. \tag{21}$$

For real values of fatigue damage at failure $0.2 < D_F < 0.8$ (see Lemaitre and Chaboche

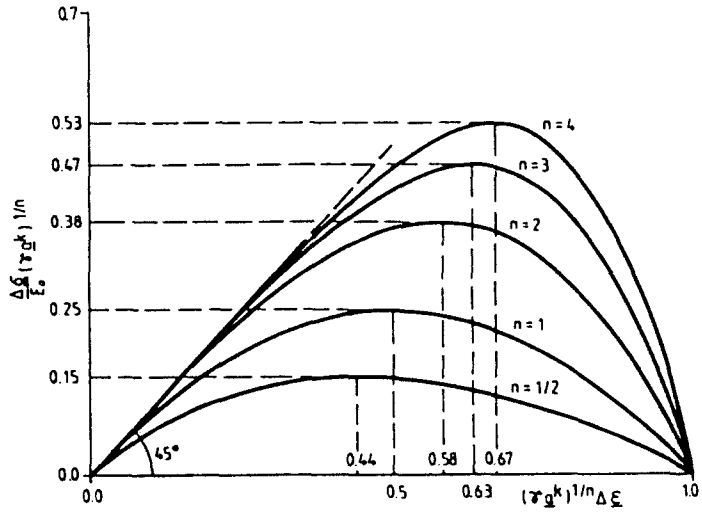

Fig. 6. Stress–strain dependence as a function of n.

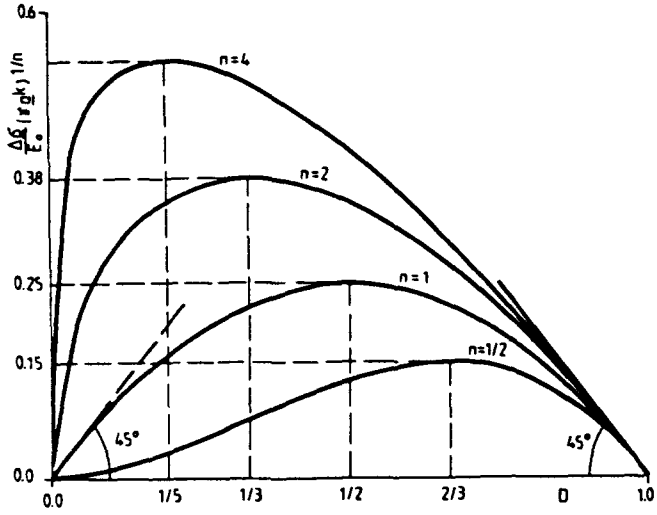

Fig. 7. Stress–damage dependence as a function of n.

(1984)); according to eqn (17) the parameter n should range between $n = 4$ and $n = 0.25$. The value of the coefficient n may be found as follows. The total strain amplitude at failure $\Delta\varepsilon_F/2$ consists of its elastic and plastic parts and obeys Manson's Law (Hertzberg, 1988):

$$\frac{\Delta\varepsilon_F}{2} = \frac{\Delta\varepsilon_{Fe}}{2} + \frac{\Delta\varepsilon_{Fp}}{2} = \frac{\sigma'_F}{E_0} N_F^b + \varepsilon'_F N_F^c, \tag{22}$$

where E_0 is modulus of elasticity of a virgin material, b and σ'_F/E_0 are the slope and one reversal intercept of the elastic part of the curve, while ε'_F is the fatigue ductility coefficient.

Since (Hertzberg, 1988, p. 503):

$$E_0 \frac{\Delta\varepsilon_{Fe}}{2} = \frac{\Delta\sigma_F}{2} = \sigma'_F N_F^b \tag{23}$$

and

$$\Delta\varepsilon = \Delta\varepsilon - \Delta\varepsilon_T = \Delta\varepsilon - \Delta\varepsilon_E, \tag{24}$$

where

$$\Delta\varepsilon_E = \frac{\Delta\sigma_E}{E_0}, \tag{25}$$

and while σ_E is the endurance limit of a real (not ideally smooth) specimen, for a stress-controlled test ($\Delta\sigma = \Delta\sigma_F$) eqns (21)–(25) produce the following result:

$$n = \frac{2\sigma'_F N_F^b - \Delta\sigma_E}{2E_0\varepsilon'_F N_F^c}. \tag{26}$$

For example, for the SAE 4340 steel (Hertzberg, 1988, p. 504); $\sigma'_F = 1200$ MPa, $\varepsilon'_F = 0.58$, $b = -0.09$, $c = -0.57$, $\sigma = 281$ MPa, assuming $E_0 = 2 \times 10^5$ MPa, depending on the stress level applied, i.e. depending on the number of cycles at failure, the coefficient n (eqn (26)) is, for example: $n = 0.4$ at $N_F = 10^4$, $n = 0.88$ at $N_F = 10^5$ and $n = 2.93$ at $N_F = 5 \times 10^6$, while the corresponding values for damage (eqn (17)) are: $D_F = 0.71, 0.53$

and 0.25. As it is seen values of $4 > n > 0.25$ estimated above and corresponding to $0.2 < D_F < 0.8$, respectively, are quite real.

From eqns (14), (17) and (18) the strain range and normalized strain range are:

$$\Delta\varepsilon = (\gamma \mathbf{a}^k)^{1/n} D^{1/n} \tag{27}$$

$$\frac{\Delta\varepsilon}{\Delta\varepsilon_F} = \mathbf{a}^{-k/n} \left(\frac{D}{D_F}\right)^{1/n}. \tag{28}$$

From eqns (16), (17) and (20) the normalized crack length is related to damage and normalized damage as:

$$\frac{n^n}{(n+1)^{n+1}} \mathbf{a}^k = (1-D)^n D \tag{29}$$

$$\left(\frac{n}{n+1}\right)^n \mathbf{a}^k = \left(1 - \frac{n}{n+1}\frac{D}{D_F}\right)^n \frac{D}{D_F}. \tag{30}$$

Definition of damage as given in (14) assumes that the initial damage is not equal to zero, since the initial crack length $\mathbf{a}_0 \neq 0$. From (29) the initial damage may be found as the solution of the following equation:

$$\frac{n^n}{(n+1)^{n+1}} \mathbf{a}_0^k = (1-D_0)^n D_0. \tag{31}$$

For small values of the initial damage $(1 - D_0) \cong 1$, such that, in that case:

$$D_0 \cong \frac{n^n}{(n+1)^{n+1}} \mathbf{a}_0^k. \tag{32}$$

Figures 8–11 present damage and strain accumulation diagrams in terms of the normalized life N/N_F and for various coefficients $\mathbf{a}_0$, q, m, k, n. For example, for given initial crack length $\mathbf{a}_0$, choosing m (typically $m = 2$) and q (typically $q = 1$), then using eqn (12), normalized crack length $\mathbf{a}$ is found as a function of the normalized life N/N_F, such as in Fig. 3. The initial damage is found from eqn (31) for a set of typical parameters n, say between $n = 1/2$ and $n = 4$. Finally, damage D, normalized damage D/D_F and normalized strain $\Delta\varepsilon/\Delta\varepsilon_F$ are found from eqns (29), (30) and (28), respectively. Unlike damage curves given in Fig. 8, normalized damage curves in Fig. 9, for the same values of parameters used, almost overlap each other (especially for small initial flaws $\mathbf{a}_0$), indicating that this could

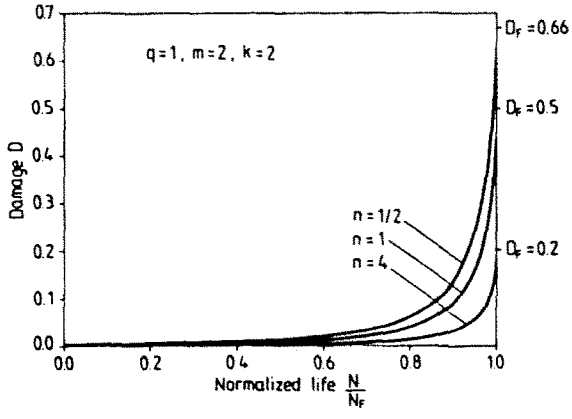

Fig. 8. Damage versus normalized life for $\mathbf{a}_0 = 0.1$.

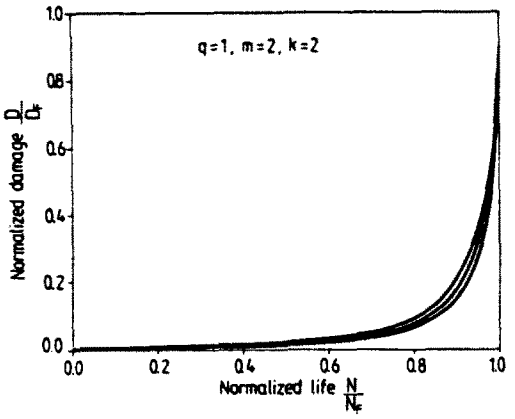

Fig. 9. Normalized damage versus normalized life for $a_0 = 0.1$.

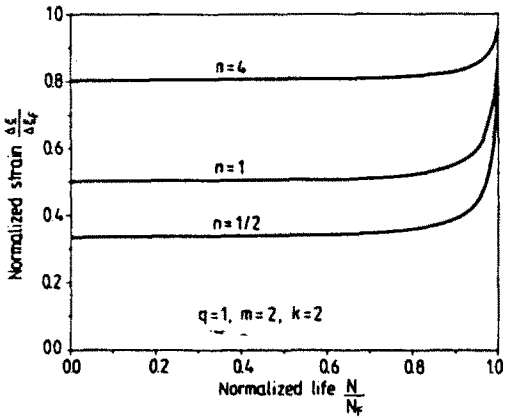

Fig. 10. Normalized strain versus normalized life for $a_0 = 0.1$.

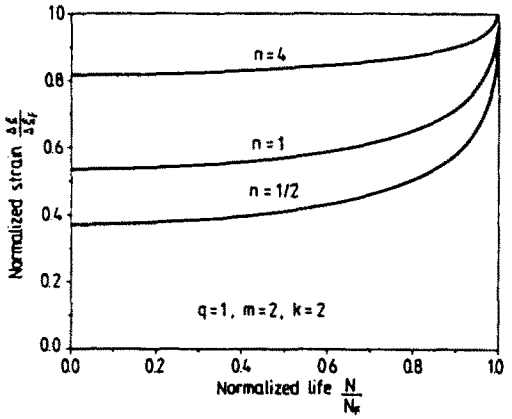

Fig. 11. Normalized strain versus normalized life for $a_0 = 0.5$.

be a better definition for damage. The shapes of damage and strain curves shown in Figs 8–11 are in a good qualitative agreement with well-known experimental results of fatigue damage (Chaboche, 1988; Socie *et al.*, 1983).

The damage model developed here includes both initiation and short crack propagation phases. Also the damage law has a nonlinear evolution and accumulation and, therefore, should be able to describe the cumulative damage under nonperiodic loading. However, a successful fatigue damage model should reflect the mean-stress influence, and this remains

to be done next. Also, values of some constants in the analytical model, such as ΔK_{th}, $\mathbf{a}_0$, m etc., and possible inclusion of the crack closure concept, are to be related to the experimental verification in further development of this model.

REFERENCES

Allen, R. J., Booth, G. S. and Jutla, T. (1988). A review of fatigue crack growth characterization by linear elastic fracture mechanics (LEFM), Part I. *Fatigue Fract. Engng Mater. Struct.* **11**, 45–69.

Brown, L. M. and Ogin, S. L. (1985). Role of internal stresses in the nucleation of fatigue cracks. In *Fundamentals of Deformation and Fracture*, pp. 501–528. Cambridge University Press, Cambridge.

Budiansky, B. and O'Connell, R. (1976). Elastic moduli of a cracked solid. *Int. J. Solids Structures* **12**, 81–97.

Cailletaud, G. and Levaillant, C. (1984). Creep–Fatigue life prediction: what about initiation? *Nucl. Engng Design* **83**, 279–292.

Chaboche, J.-L. (1988). Continuum damage mechanics (Part I—General concepts, and Part II—Damage growth, crack initiation and crack growth). *J. Appl. Mech.* **55**, 59–72.

Collins, J. A. (1981). *Failure of Materials in Mechanical Design*. Wiley, New York.

El Haddad, M. H., Topper, T. H. and Smith, K. N. (1979). Prediction of non-propagating cracks. *Engng Fract. Mech.* **11**, 573–584.

Hertzberg, W. R. (1988). *Deformation and Fracture Mechanics of Engineering Materials*. Wiley, New York.

Hobson, P. D. (1982). The formulation of a crack growth equation for short cracks. *Fatigue Engng Mater. Struct.* **5**, 323–327.

Hua, C. T. and Socie, D. F. (1984). Fatigue damage in 1045 Steel under constant amplitude biaxial loading. *Fatigue Engng Mater. Struct.* **7**, 165–179.

Kitagawa, H. and Takahashi, S. (1976). Applicability of fracture mechanics to very small cracks or the cracks in the early stage. *Proc. Int. Conf. on the Mechanical Behaviour of Materials (ICM2)*, American Society of Metals, pp. 627–631.

Kitagawa, H., Takahashi, S., Suh, C. M. and Miyashita, S. (1979). Quantitative analysis of fatigue process—microcracks and slip lines under cyclic strains. *ASTM STP* **675**, 420–449.

Krajcinovic, D. and Lemaitre, J. (1987). *Continuum Damage Mechanics Theory and Applications*. Springer, Wien.

Laws, N. and Brockenbrough, J. R. (1987). The effect of micro-cracks systems on the loss of stiffness of brittle solids. *Int. J. Solids Structures* **23**, 1247–1268.

Lemaitre, J. and Chaboche, J.-L. (1984). *Mechanique des Matériaux Solides*. Dunod, Paris.

Liu, L. C., Tay, Y. K. and Fong, H. S. (1990). Fatigue damage and crack nucleation mechanisms at intermediate strain amplitudes. *Acta Metall. Mater.* **38**, 595–601.

Liu, H. W. and Liu, D. (1982). Near threshold fatigue crack growth behaviour. *Scripta Metall.* **16**, 595–600.

Liu, H. W. and Liu, D. (1984). A quantitative analysis of structure sensitive fatigue crack growth in steels. *Scripta Metall.* **18**, 7–12.

Magnin, T., Ramade, C., Lepinoux, J. and Kubin, L. P. (1989). Low-cycle fatigue damage mechanisms of f.c.c. and b.c.c. polycrystals: homologous behaviour? *Mater. Sci. Engng* **A118**, 41–51.

Miller, K. J. (1982). The short crack problem. *Fatigue Engng Mater. Struct.* **5**, 223–232.

Miller, K. J. and de los Rios, E. R. (1986). *Proceedings: The Behaviour of Short Fatigue Cracks*. Mechanical Engineering Publications, London.

Miller, K. J. (1987). The behaviour of short fatigue cracks and their initiations—Parts I and II. *Fatigue Fract. Engng Mater. Struct.* **10**, 75–113.

Navaro, A. and de los Rios, E. R. (1987). A model for short fatigue crack propagation with an interpretation of the short–long crack transition. *Fatigue Fract. Engng Mater. Struct.* **10**, 169–186.

Pašić, H. (1990). High-cycle fatigue damage in polycrystalline materials. Scientific report, JRC EURATOM—Institute for Advanced Materials, Ispra, Italy.

Polak, J. and Liskutin, P. (1990). Nucleation and short crack growth in fatigued polycrystalline copper. *Fatigue Fract. Engng Mater. Struct.* **13**, 119–133.

Popelar, C. H. and Hoagland, R. G. (1986). On the nature of crack propagation and arrest in a damaging material. *Engng Fract. Mech.* **23**, 131–144.

Socie, D. F., Fash, J. W. and Leckie, F. A. (1983). A continuum damage model for fatigue analysis of cast iron. *ASME Conf. on Life Predictions*, Albany, New York, pp. 59–64.

Suh, C. M., Yuuki, R. and Kitagawa, H. (1985). Fatigue microcracks in a low carbon steel. *Fatigue Fract. Engng Mater. Struct.* **8**, 193–203.

Suh, C. M., Lee, J. J. and Kang, J. G. (1990). Fatigue microcracks in type 304 stainless steel at elevated temperature. *Fatigue Fract. Engng Mater. Struct.* **13**, 487–496.

Suresh, S. and Ritchie, R. O. (1984). Propagation of short fatigue cracks. *Int. Metals Rev.* **29**, 445–475.

Tanaka, K., Nakai, Y. and Yamashita, M. (1981). Fatigue growth threshold of small cracks. *Int. J. Fract.* **17**, 519–533.

Xiulin, Z. (1987). A simple formula for fatigue crack propagation and a new method for the determination of ΔK. *Engng Fract. Mech.* **27**, 465–475.

Yoder, G. R., Coolley, L. A. and Crooker, T. W. (1982). On microstructural control of near-threshold fatigue crack growth in 7000-series aluminum alloys. *Scripta Metall.* **16**, 1021–1025.